Langmuir

Article

pubs.acs.org/Langmuir

Equilibrating Immigration and Anthracene-Maleimide-Based Diels–Alder-Trapping of Octylmaleimide in Mixed Photo-Cross-Linked Polymer Micelles

Yan Liu, Min Tian, Huan Chang, Jinqiang Jiang,* Xiangyang Yan, Zhaotie Liu, and Zhongwen Liu

Key Laboratory of Applied Surface and Colloid Chemistry, Ministry of Education, School of Chemistry and Chemical Engineering, Shaanxi Normal University, Xi'an, Shaanxi China, 710062

Supporting Information

ABSTRACT: It is possible that the hydrophobic guest within amphiphilic polymer micelles may leak out and be captured by other species before polymer micelles adhere to the desired focus because of the complexity in an actual release procedure, rendering the reduced efficiency of the nanocarrier system. To describe such a scenario, two water-soluble fluorescent amphiphilic random copolymers of **PAV** and **PAA** with photo-cross-linkable coumarin and anthracene pendants, respectively, were chosen to investigate the equilibrating immigration and maleimide-anthracene-based Diels–Alder-trapping of hydrophobic octylmaleimide guest from one type of photo-cross-linked polymer micelles of $\mathbf{PAV}_{85\%}$ to another of $\mathbf{PAA}_{66\%}$ in aqueous solution using the emission and absorption spectra techniques.

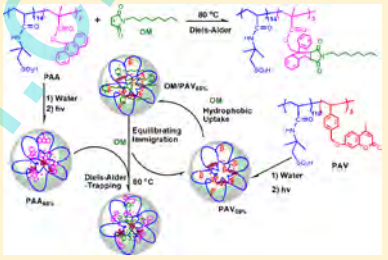

1. INTRODUCTION

Over the last few decades, amphiphilic polymer micelles have emerged as viable platforms for the encapsulation and delivery of hydrophobic molecules in a nanocarrier system.[1−7] For this purpose, polymer micelles must efficiently encapsulate hydrophobic guests until they adhere to the desired focus.[4,8,9] It is known that the inherent loading capacity of polymer micelles in aqueous solution can be fine-tuned by slight variations in amphiphilic polymer structure parameters, such as hydrophobic content in amphiphilic polymer. However, the hydrophobic guest in micellar aqueous solution itself is just an indicator of the thermodynamic distribution between polymer micelles and the bulk solvent.[10−14] This means that hydrophobic guests in nanocarriers may leak out after being administrated in the body due to the extreme dilution or other factors, rendering any strategy for site-specific transport of polymer micelles useless.[15−18] Therefore, understanding the thermodynamic distribution of hydrophobic encapsulation can provide some crucial implications to nanocarriers.

Thayumanavan and co-workers have established an elegant method to evaluate the stability of drug delivery vehicles. They succeeded in evaluating the dynamic exchange of hydrophobic fluorescent molecules within nanoassemblies in aqueous solutions using a fluorescence resonance energy transfer (FRET)-based method.[18−20] However, it is also possible that the hydrophobic guest may be captured by other species before polymer micelles adhere to the desired focus because of the complexity in an actual release procedure, also resulting in the reduced efficiency of nanocarrier system. Herein, in our continuing efforts to develop photo-cross-linkable amphiphilic polymers, we sought to describe such a scenario by incorporation of the maleimide-based fluorescence quenching effect within photo-cross-linked fluorescent polymer micelles to trace the hydrophobic guest immigration and the maleimide-anthracene-based Diels–Alder addition to perform the thermal-induced guest trapping in a mixed micellar system.

As schematically shown in Figure 1, two photo-cross-linkable fluorescent amphiphilic random copolymers of **PAV** and **PAA**, that is, poly[(2-acrylamido-2-methylpropanesulfonic acid-*co*-(7-(4-vinyl-benzyloxyl)-4-methylcoumarin)] and poly[(2-acrylamido-2-methylpropanesulfonic acid)-*co*-(anthracene methyl methacrylate)], were independently self-assembled into nanoaggregates in aqueous solution and irradiated to form photo-cross-linked polymer micelles of $\mathbf{PAV}_{85\%}$ and $\mathbf{PAA}_{66\%}$, respectively. In addition, the fluorescence quencher of *n*-octylmaleimide (OM) was chosen as hydrophobic guest to be uploaded into $\mathbf{PAV}_{85\%}$ polymer micelles. Then $\mathbf{OM/PAV}_{85\%}$ was chosen as a maleimide source to mixed with $\mathbf{PAA}_{66\%}$ to form the mixed micellar systems, resulting in the equilibrating immigration of OM molecules from photo-cross-linked polymer micelles of $\mathbf{PAV}_{85\%}$ into $\mathbf{PAA}_{66\%}$. Furthermore, when the mixed system was heated at 80 °C, the OM molecules would be trapped by $\mathbf{PAA}_{66\%}$ polymer micelles because of the thermal-induced anthracene-maleimide Diels–Alder addition.

2. EXPERIMENTAL SECTION

2.1. Materials. 2, 2-Azoisobutyronitrile (AIBN) was purified by recrystallization from 95% ethanol. *n*-Octylmaleimide (OM), 2-acrylamido-2-methylpropanesulfonic acid (AMPS), 4-vinylbenzyl chloride, methacryloyl chloride, 9-anthracenemethanol, and 4-methylumbelliferone were purchased from Aladdin and used without further purification. Ultrapure water was prepared utilizing a FDY-1002–UV-

Received: October 7, 2014
Revised: November 18, 2014
Published: November 25, 2014

   dx.doi.org/10.1021/la503971q | *Langmuir* 2014, 30, 14782−14788

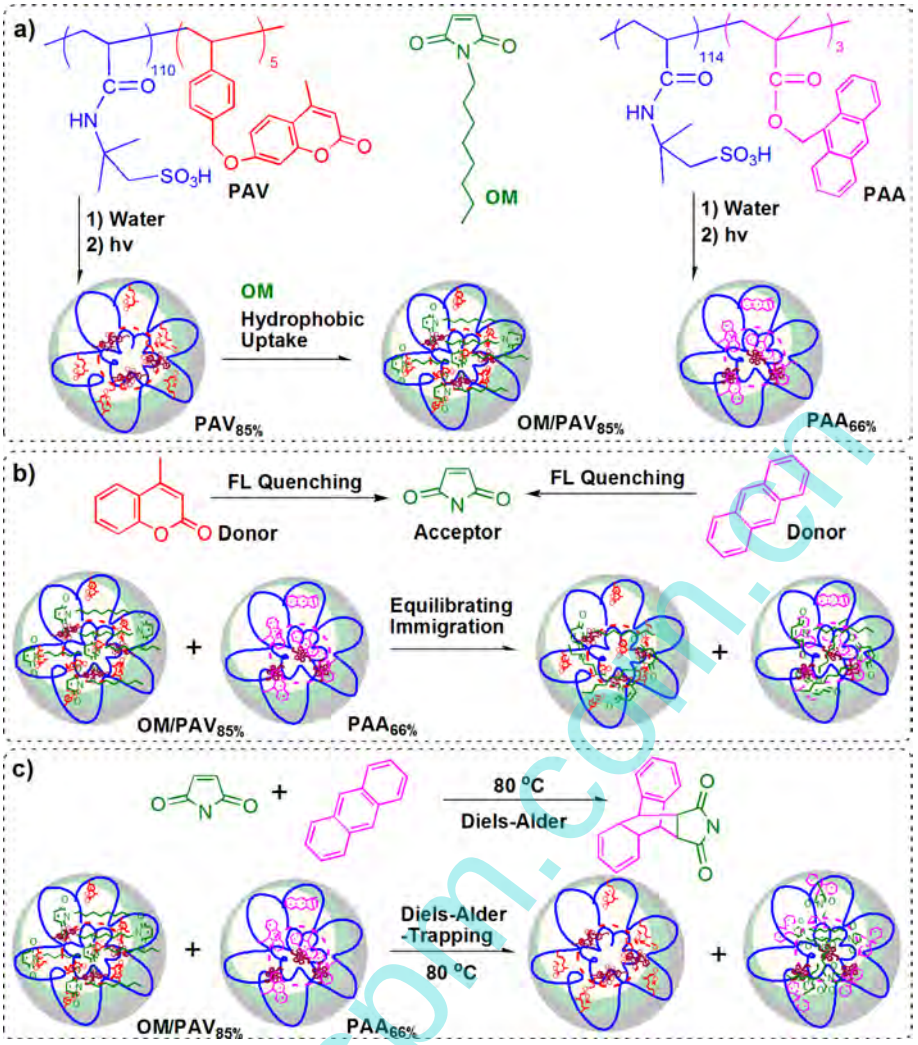

Figure 1. (a) Schematic structures of two photo-cross-linkable fluorescent amphiphilic copolymers of **PAV** and **PAA** and the hydrophobic guest of *n*-octylmaleimide (OM). (b) Equilibrating immigration of OM molecules from **OM/PAV**$_{85\%}$ to **PAA**$_{66\%}$ in the mixed micellar systems. (c) Thermal-induced Diels–Alder-trapping of hydrophobic OM guest in mixed micellar systems.

P purification system. The anthracene methyl methacrylate (AM) and 7-(4-vinyl-benzyloxyl)-4-methylcoumarin (VBC) were prepared according to our previous works.[21,22]

2.2. Characterization. ^{1}H NMR (400 MHz) spectra were investigated by a Bruker spectrometer with d_6-DMSO as solvent.

GPC was performed using a Waters system with DMF as eluent (0.5 mL min^{-1}) and polystyrene as standard.

Absorption spectra were measured with an Evolution 220 spectrophotometer (Thermo Fish Instrument Co., Ltd.).

Fluorescence emission spectra were measured with a PTI fluorescence master system. The slit width was maintained at 0.75 nm for excitation and 0.50 nm for emission, respectively. The fluorescence spectra were taken with λ_{ex} at 353 nm.

Dynamic light scattering (DLS) measurements were performed with a Malvern Nano-ZS90 instrument (Malvern, U.K.) to determine the average diameter and size distribution of micelles at room temperature.

AFM images of micelles were observed by a CSPM5500A scanning probe microscope system (Bejing Nano-Instruments Co., Ltd.) in the tapping mode. Samples were prepared by dropping the micellar solution onto mica sheets and drying the sheets at room temperature overnight.

The photo-cross-linking reaction of anthracene and coumarin pendants, respectively, was achieved by the irradiation of 365 nm LED light (Shanghai Huave Info-Tech Co., Ltd.) with mild stirring, the distance between the solution and the spotlight was about 1.0 cm.

2.3. Synthesis of Photo-Cross-Linkable Fluorescent Amphiphilic Random Copolymer of PAA. To a 50 mL ampule, AIBN (0.028 g, 0.17 mmol), AMPS (8.300 g, 40 mmol), AM (0.582 g, 2.1 mmol), and DMF/H_2O (30 mL, V/V = 3/1) were quickly added. Then, the mixture was degassed, and filled with nitrogen. After 30 min stirring at room temperature, the ampule was placed in a preheated oil bath (95 °C) for 30 h. The amphiphilic polymer of **PAA** was collected by precipitation twice into diethyl ether. The crude product was dialyzed against ultrapure water while stirring for 3 days; water was frequently refreshed (every 2 h during day time). Finally, the amphiphilic polymer was dried to constant weight under vacuum freeze drying condition. Yield: 70%. Mn = 2.44 × 10^4 g mol^{-1}. M_w/M_n = 1.20 (GPC). ^{1}H NMR (DMSO), δ (ppm): 8.35 (s, –NH–), 7.70–7.06 (m, aromatic H), 6.19 (s, –C(=O)–CH), 5.13 (s, –CH_2O–). **PAA** was further estimated to compose of 114 AMPS and 3 AM units according to the calibration curve of AM in DMF (see S1 in the Supporting Information).

2.4. Synthesis of Photo-Cross-Linkable Fluorescent Amphiphilic Random Polymer of PAV. To a 50 mL ampule, AIBN (0.023 g, 0.14 mmol), AMPS (6.218 g, 30 mmol), VBC (0.792 g, 2.7 mmol), and DMF/H_2O (30 mL, V/V = 3/1) were quickly added. The synthetic process and post-treatment were same with the synthesis of **PAA**. Yield: 70%. Mn = 2.42 × 10^4 g mol^{-1}. M_w/M_n = 1.20 (GPC). ^{1}H NMR (DMSO), δ (ppm): 8.32 (s, –NH–), 8.00–7.17 (m, aromatic

dx.doi.org/10.1021/la503971q | Langmuir 2014, 30, 14782–14788

H), 6.86 (s, $-CH_2O-$). **PAV** was further estimated to be composed of 110 AMPS and 5 VBC units according to the calibration curve of VBC in DMF (see S2 in the Supporting Information).

2.5. Preparation of Photo-Cross-Linked Polymer Micelles in Aqueous Solution. The calculated amount of amphiphilic copolymers of **PAV** and **PAA** were independently and directly dissolved in aqueous solution to a concentration of 5.00 mg mL^{-1} and then conveniently photo-cross-linked using 365 nm LED irradiation to form photo-cross-linked polymer micelles of $\mathbf{PAV}_{85\%}$ and $\mathbf{PAA}_{66\%}$, respectively. The percentage numbers here corresponded to the cross-linking densities, which were evaluated according to the characteristic absorption intensity changes of coumarin at 320 nm and anthracene at 390 nm (see Figure 2a), respectively.

The size distributions of these polymer micelles (0.25 mg mL^{-1}) were analyzed by DLS instrument at room temperature, and the micellar morphologies were observed with AFM images.

2.6. Equilibrating Immigration of OM Molecules in the Mixed Micellar Systems. Calculated amount of **PAA** (50.00 mg) and *n*-octylmaleimide (15.00 mg) were added into water (10 mL) with mild stirring for 48 h, and then the polymer aqueous solution was transferred carefully into another ampule after standing for 2 h. Additionally, 0.1 mL of polymer aqueous solution was mixed with 1.90 mL of 9-anthracenemethanol DMF solution (0.31 mg mL^{-1}) in the fluorescence cuvette and heated to 80 °C for 2 h to trigger the anthracene-maleimide Diels–Alder addition while stirring, resulting in the estimation of the encapsulated OM molecules in **PAA** aqueous solution according to the decreasing absorption band intensity at 390 nm before and after heating. Then, calculated amount of **PAA** and water was added into the OM loaded polymer micelles with mild stirring for another 48 h to prepare the specified weight percent OM loaded polymer micelles of **PAA** (4.00 mg mL^{-1}). Furthermore, the other three polymer micelles of $\mathbf{OM/PAA}_{66\%}$, **OM/PAV** and $\mathbf{OM/PAV}_{85\%}$ with different weight percent OM encapsulation were prepared following the same procedure, and polymer concentrations were kept at 4.00 mg mL^{-1}.

These OM loaded polymer micelles were checked with absorption and emission spectra instruments while polymer concentration was diluted to 0.25 mg mL^{-1} with water.

OM equilibrating immigration experiments were achieved by monitoring the fluorescence spectra changes (λ_{ex} = 353 nm) of two sets of mixed micellar systems every 10 min for about 2 h. For set one (S_1), 0.75 mL of 0.5, 1.0, and 2.0 wt % OM loaded micelles of $\mathbf{PAV}_{85\%}$ (0.50 mg mL^{-1}) was mixed with 0.75 mL $\mathbf{PAA}_{66\%}$ (0.50 mg mL^{-1}) in the fluorescence cuvette to form three mixed micellar systems of $S_{1\text{-}1}$, $S_{1\text{-}2}$ and $S_{1\text{-}3}$, respectively; for set two (S_2), 2.0 wt % of OM loaded micelles of $\mathbf{PAV}_{85\%}$ (1.00, 2.00, 4.00 mg mL^{-1}) was mixed with $\mathbf{PAA}_{66\%}$ (0.50 mg mL^{-1}) in the same volume and denoted as $S_{2\text{-}1}$, $S_{2\text{-}2}$, and $S_{2\text{-}3}$, respectively.

2.7. Diels–Alder-Trapping of OM Molecules in Mixed Micellar Systems upon Heating. The above six mixed micellar systems were further heated from 25 °C to 80 °C within 1 min, then kept at 80 °C for 2 h with mild stirring, resulting in the Diels–Alder addition between OM molecules and anthracene pendants within $\mathbf{PAA}_{66\%}$. The heating procedures were monitored with absorption spectra and emission spectra with λ_{ex} at 353 nm.

3. RESULTS AND DISCUSSION

3.1. Preparation of Photo-Cross-Linked Polymer Micelles in Aqueous Solution. Coumarin and anthracene are well-known for their characteristic photodimerization reactions, which have been widely investigated for the application of photoresponsive materials.[4,23−35] Furthermore, polymer micelles can be stabilized by the photodimerization of coumarin or anthracene moieties incorporated in amphiphilic polymers.[4]

As designed, two photo-cross-linkable fluorescent moieties of coumarin and anthracene were introduced into the water-soluble amphiphilic polymers of **PAV** and **PAA**, respectively. The polymers were independently dissolved in aqueous solution to form nanoaggregates and then photo-cross-linked to a certain degree with 365 nm light irradiations. Figure 2

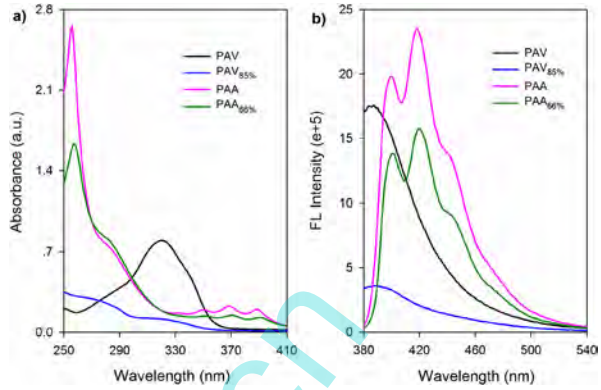

Figure 2. (a) Absorption spectra of **PAV** (0.25 mg mL^{-1}) and **PAA** (0.25 mg mL^{-1}) in aqueous solution before and after photo-cross-linking. (b) Fluorescence spectra (λ_{ex} = 353 nm) of **PAV** (0.25 mg mL^{-1}) and **PAA** (0.25 mg mL^{-1}) in aqueous solution before and after photo-cross-linking.

showed the absorption and emission spectra of **PAV** and **PAA** before and after photo-cross-linking. As shown in Figure 2, polymer micelles in aqueous solution of **PAV** afforded a broad absorption band centered at 320 nm (log ε = 4.19), which decreased significantly after the photodimerization of coumarin pendants. On the other hand, **PAA** showed a highest absorption band around 256 nm (log ε = 4.94) with a shoulder at 285 nm and a series of vibrationally spaced absorption structures at 335, 353, 370, and 390 nm (finger-like absorption bands), whose intensities (except for 285 nm) decreased after the photo-cross-linking reaction of anthracene pendants. As shown in Figure 2b, **PAV** polymer aqueous solutions showed a characteristic broad emission peak around 385 nm, which was greatly suppressed after photo-cross-linking; **PAA** showed a multiple emission band peaking at 399, 419, and 440 nm, whose intensities decreased by a third after the photo-cross-linking. These results indicated the different inherent electron properties of coumarin and anthracene chromophores in aqueous polymer micelles of **PAV** and **PAA**, respectively.

The size distributions of polymer nanoaggregates in aqueous solution before and after photo-cross-linking were monitored by DLS instrument. As shown in Figure 3a, the average size of

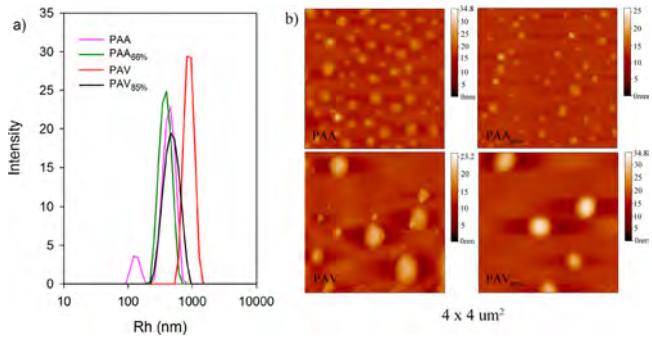

Figure 3. (a) Size distributions of polymer micelles of **PAV** (0.25 mg mL^{-1}) and **PAA** (0.25 mg mL^{-1}) in aqueous solution before and after photo-cross-linking. (b) AFM images for polymer micelles of **PAV** and **PAA** before and after photo-cross-linking.

dx.doi.org/10.1021/la503971q | *Langmuir* 2014, 30, 14782−14788

PAV (~920 nm) and **PAA** (~460 nm) decreased significantly to ~600 nm and ~400 nm after the photo-cross-linking of coumarin and anthracene pendants, respectively, revealing the photo-cross-linking effect in polymer micelles. Furthermore, these polymer micelles were also visualized with nanospheres by AFM images (see Figure 3b). The average diameter measured by AFM was much smaller than those measured by DLS at 25 °C. This discrepancy in size could be attributed to the fact that DLS data directly reflected the dimension of polymer nanoaggregates in aqueous solution, where hydrophilic chains were well dispersed in water with hydrophobic components loosely associating within water-soluble amphiphilic polymer micelles.

3.2. Equilibrating Immigration of OM Molecules in Mixed Micellar Systems. Maleimide is known as one of the most efficient electron acceptors to electron-rich moieties, such as coumarin and anthracene, resulting in the fluorescent emission reduction of the donor chromophores.[36−38] As discussed above, because the coumarin and anthracene pendants in polymer micelles had different inherent electron properties, the resultant fluorescence quenching effect of OM to polymer micelles of **PAA** and **PAV** before and after photo-cross-linking should have various fluorescence quenching behaviors.

In addition, as shown in Figure 4a, when the hydrophobic electron acceptor of OM was encapsulated into polymer micelles of $\mathbf{PAA}_{66\%}$, the multiple fluorescence emission band covering 380−540 nm intervals decreased gradually as a function of OM weight percentage without any significant peak shift, resulting in the evaluation of quenching effect of **OM/PAA** by the normalized emission intensities at 419 nm. Thus, the bigger the normalized *I*, the less quenching effect of OM to fluorescent polymer micelles. As shown in Figure 4b, at the used conditions, the normalized *I* of **OM/PAA** and **OM/PAV** polymer aqueous solutions decreased linearly with a linear fit slope of −0.0331 and −0.0067, respectively, indicating the greater fluorescence quenching effect of **OM/PAA** than **OM/PAV**. Interestingly, the fluorescence quenching effect of two photo-cross-linked polymer micelles of $\mathbf{OM/PAA}_{66\%}$ and $\mathbf{OM/PAV}_{85\%}$ were obviously greater than the corresponding precursor polymer micelles of **OM/PAA** and **OM/PAV** at lower OM weight percentage, then significantly suppressed with the increasing weight percentage of OM encapsulation, respectively. This could be attributed to two factors: one was that the photo-cross-linked polymer micelles contained fewer chromophores of anthracene and coumarin than the corresponding precursor of **PAA** and **PAV**, respectively; another was the "incarceration" effect generated by the photo-cross-linking, which could stabilize the polymer micellar structure and encapsulate more OM guest molecules within photo-cross-linked polymer micelles. Furthermore, $\mathbf{OM/PAA}_{66\%}$ showed a much greater exponential decay as a function of OM weight percent than $\mathbf{OM/PAV}_{85\%}$, resulting in the ever increasing gaps of normalized *I* between OM loaded polymer micelles of $\mathbf{PAA}_{66\%}$ and $\mathbf{PAV}_{85\%}$, respectively.

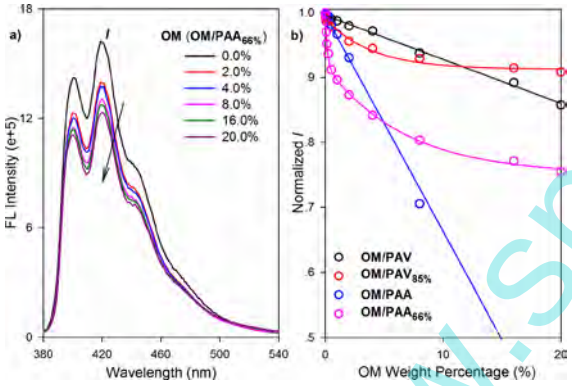

Figure 4. (a) Fluorescence spectra (λ_{ex} = 353 nm) of OM loaded polymer micelles of $\mathbf{PAA}_{66\%}$ (0.25 mg mL^{-1}). (b) Plots of normalized *I* vs OM weight percentage in polymer micelles of **PAV** (0.25 mg mL^{-1}) and **PAA** (0.25 mg mL^{-1}) before and after photo-cross-linking.

The key motivation of OM immigration in mixed micellar system significantly depended on the thermodynamic equilibration of OM between two photo-cross-linked polymer micelles of $\mathbf{PAA}_{66\%}$ and $\mathbf{PAV}_{85\%}$. Thus, if $\mathbf{OM/PAV}_{85\%}$ were chosen as the maleimide source to be mixed with nonloaded $\mathbf{PAA}_{66\%}$, the OM molecules would immigrate from $\mathbf{PAV}_{85\%}$ into $\mathbf{PAA}_{66\%}$ because of the great concentration difference of OM in two polymer micelles, and the immigration speed would be slowed down along with the decreasing concentration difference. In addition, along with the increasing weight percentage of OM within $\mathbf{PAV}_{85\%}$, more OM molecules would leak into $\mathbf{PAA}_{66\%}$ polymer micelles, resulting in the greater decrease in fluorescence intensity of the mixed system. As designed, the same volume of $\mathbf{OM/PAV}_{85\%}$ and $\mathbf{PAA}_{66\%}$ (0.50 mg mL^{-1}) were mixed together and monitored with fluorescence emission spectra over the mixing time. The mixed micellar systems were classified with set one (S_1) according to the weight percentage (0.5%, 1.0%, and 2.0%) of OM encapsulated in $\mathbf{PAV}_{85\%}$ (0.50 mg mL^{-1}) and set two (S_2) with the increasing polymer concentration (1.00, 2.00, and 4.00 mg mL^{-1}) of 2.0 wt % OM loaded micelles of $\mathbf{PAV}_{85\%}$, and denoted as $S_{1\text{-}1}$, $S_{1\text{-}2}$, $S_{1\text{-}3}$, $S_{2\text{-}1}$, $S_{2\text{-}2}$, and $S_{2\text{-}3}$, respectively. As shown in Figure 5a, the multiple fluorescence emission bands of $S_{1\text{-}3}$ covering 380−600 nm intervals decreased slightly but significantly as a function of mixing time, evidently confirming the immigration of OM molecules from $\mathbf{PAV}_{85\%}$ into $\mathbf{PAA}_{66\%}$ and resulting in the evaluation of OM molecule immigration by the normalized emission intensity at 419 nm. Figure 5b showed the time-dependent *I* values of mixed micellar systems in 2 h. The OM molecule immigration was indicated by a gradual exponential decay of the normalized *I*. It was clearly shown that the immigration of OM from $\mathbf{PAV}_{85\%}$ into $\mathbf{PAA}_{66\%}$ was propor-

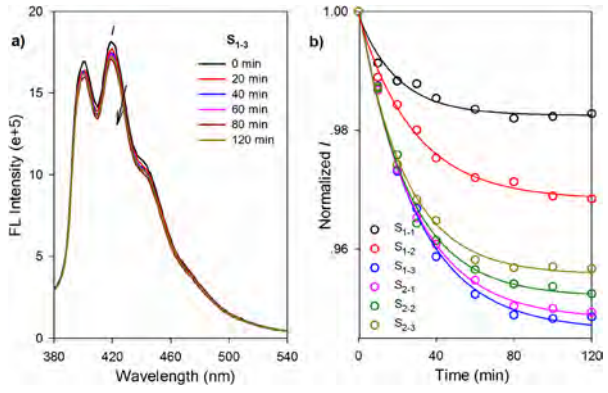

Figure 5. (a) Fluorescence spectra (λ_{ex} = 353 nm) of mixed micellar system of $S_{1\text{-}3}$. (b) Plots of normalized *I* of two set of mixed micellar systems as a function of mixing time.

dx.doi.org/10.1021/la503971q | *Langmuir* 2014, 30, 14782−14788

tionally accelerated as the increasing amount of OM encapsulated in $\mathbf{PAV}_{85\%}$ polymer micelles and leveled off after 60, 80, and 100 min for $S_{1\text{-}1}$, $S_{1\text{-}2}$ and $S_{1\text{-}3}$, respectively. The normalized I changes of S_2 afforded almost the same decrease with $S_{1\text{-}3}$ in the downhill stage in the initial 20 min mixing time and then slightly accelerated as a function of the micellar ratio of $\mathbf{OM/PAV}_{85\%}$ to $\mathbf{PAA}_{66\%}$.

3.3. Maleimide-Anthracene-Based Diels–Alder-Trapping of OM Molecules in Mixed Micellar Systems upon Heating. Other than the photodimerization upon light irradiation, another more intriguing aspect of anthracene is the ability to undergo both thermal and photochemical Diels–Alder additions with a variety of dienophiles,[39] especially maleimide,[40,41] across the 9 and 10 positions, resulting in the break of its conjugated structure, which appears to be governed much more by temperature. However, higher temperatures above 90 °C can favor the retro Diels–Alder reaction. Thus, when to 80 °C, OM molecules will not only immigrate from $\mathbf{PAV}_{85\%}$ into $\mathbf{PAA}_{66\%}$ but also be trapped by anthracene pendants through the anthracene-maleimide-based Diels–Alder addition, which we called "Diels–Alder-trapping" of OM guest in mixed micellar systems.

As shown in Figure 6a, the absorption spectra of two set of mixed micellar systems and $\mathbf{PAA}_{66\%}$ showed very similar weak shoulders at 370 and 390 nm belonging to the characteristic absorption bands of anthracene; furthermore, the characteristic band shape and intensity at 390 nm of six mixed micellar systems almost remained unchanged as against that of $\mathbf{PAA}_{66\%}$ despite of the different micellar ratio between $\mathbf{OM/PAV}_{85\%}$ and $\mathbf{PAA}_{66\%}$, which helped to trace the maleimide-anthracene Diels–Alder addition by monitoring the absorption spectra changes. It was understandable that the Diels–Alder addition would increase along with the increasing OM molecules in the mixed system. As shown in Figure 6b, the absorption band at 390 nm of $S_{1\text{-}3}$ decreased obviously during the heating procedure, indicating the ongoing maleimide-anthracene Diels–Alder addition within polymer micelles of $\mathbf{PAA}_{66\%}$. Furthermore, as shown in Figure 6c, the absorption spectra of $\mathbf{OM/PAV}_{85\%}$ almost showed no changes during the heating procedure. Therefore, the normalized intensity changes at 390 nm (I_{390}) of anthracene can be chosen to evaluate the OM molecule trapping effect in mixed micellar systems. As shown in Figure 6d, the time-dependent I_{390} values of $S_{1\text{-}1}$, $S_{1\text{-}2}$, and $S_{1\text{-}3}$ decreased vertically to 0.967, 0.954, and 0.938 during the initial 1 min heating procedure from 25 °C to 80 °C and then decreased gently with a slope of −0.0001, −0.0002, and −0.0003 during the other 2 h heating period at 80 °C, respectively, ascribing to a possibility of anthracene-maleimide Diels–Alder addition in the initial heating stage. S_2 afforded three similar decrease of normalized I_{390} values during the initial 1 min heating stage, then presented faster exponential decay with the increasing micellar ratio of $\mathbf{OM/PAV}_{85\%}$ during the other 2 h heating time.

Furthermore, the resulting succinimide groups of maleimide-anthracene addition would no longer exhibit a strong quenching effect. Thus, the OM trapping procedure could also be monitored by fluorescent emission instrument. As shown in Figure 7a, the multiple emission band of $S_{1\text{-}3}$ was not always weakening during the heating procedure, which plummeted down at the beginning and then increased gradually upon further heating at 80 °C. As shown in Figure 7b, the time-dependent I values of S_1 decreased vertically to 0.900, 0.850, and 0.765 during the initial 1 min heating procedure, respectively. Then $S_{1\text{-}1}$ showed almost unchanged I values during the other 2 h heating period at 80 °C, indicating that all of the OM molecules may be trapped within the initial 1 min heating procedure. $S_{1\text{-}3}$ afforded an quicker increasing I values than $S_{1\text{-}2}$ as a result of more OM molecules being encapsulated in the mixed micellar system. S_2 also afforded similar I changes with the lowest at 0.740, 0.716, and 0.696 in the initial stage and the final at 0.834, 0.806, and 0.736 along with the increasing micellar weight ratio of $\mathbf{OM/PAV}_{85\%}$. These "vertical

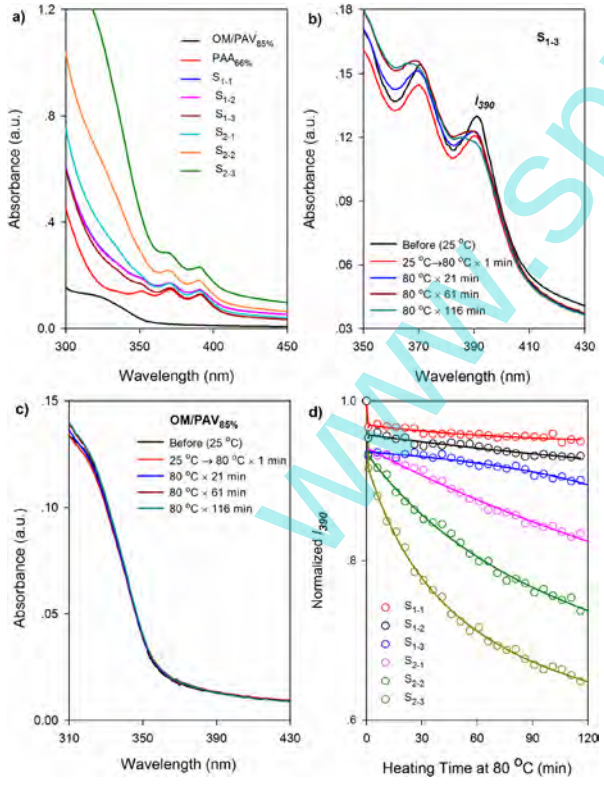

Figure 6. (a) Absorption spectra of $\mathbf{OM/PAV}_{85\%}$ (0.005, 0.25 mg mL^{-1}), $\mathbf{PAA}_{66\%}$ (0.25 mg mL^{-1}), and two sets of mixed micellar systems. (b) Absorption spectra changes of $S_{1\text{-}3}$ during the heating procedure. (c) Absorption spectra changes of $\mathbf{OM/PAV}_{85\%}$ (0.005, 0.25 mg mL^{-1}) during the heating procedure. (d) Plots of normalized I_{390} of the mixed micellar systems as a function of heating time.

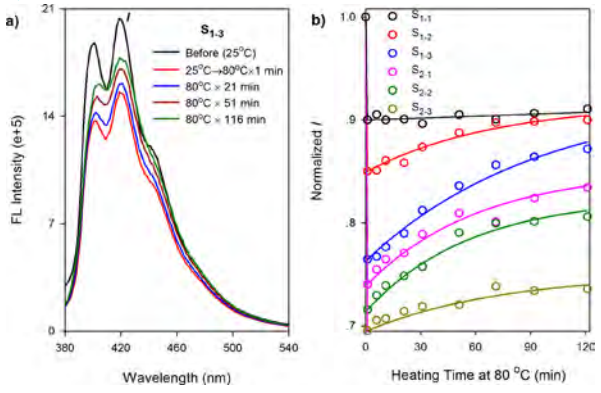

Figure 7. (a) Fluorescence spectra changes (λ_{ex} = 353 nm) of $S_{1\text{-}3}$ during the heating procedure. (b) Plots of normalized I at 419 nm of mixed micellar systems as a function of heating time.

dx.doi.org/10.1021/la503971q | Langmuir 2014, 30, 14782–14788

down−gradual up" changes of normalized I were well consistent with the absorption spectra analysis in Figure 6d. In addition, from the viewpoint of molar ratio of OM to anthracene in mixed micellar systems ($S_{1\text{-}2}$ corresponding to equimolar OM and anthracene), these results indicated that many of OM molecules in mixed micellar systems of S_2 were not trapped by $\mathbf{PAA}_{66\%}$ polymer micelles during the 2 h heating procedure at 80 °C.

4. CONCLUSIONS

In summary, two types of photo-cross-linked fluorescent polymer micelles were chosen to describe the hydrophobic guest immigration and molecular trapping in mixed micellar systems. Methods of absorbance and fluorescence spectra, DLS, and AFM were applied. The results showed that OM molecules could present different fluorescence quenching effects to polymer micelles of $\mathbf{PAV}_{85\%}$ and $\mathbf{PAA}_{66\%}$, respectively, resulting in the evaluation of OM molecular immigration from $\mathbf{PAV}_{85\%}$ into $\mathbf{PAA}_{66\%}$ by tracing the evolution of fluorescence quenching over the mixing time. The OM trapping analysis by absorption and emission spectra showed a possibility of anthracene-maleimide Diels−Alder addition in the initial 1 min heating stage; however, many of the OM molecules were still not trapped by $\mathbf{PAA}_{66\%}$ polymer micelles during the 2 h heating procedure. Since the guest employed model the hydrophobic nature of drug molecules, this feature can provide some implications to the potential nanocarrier leakage and also renders photo-cross-linked polymers to be of great interest for controlled release applications in the area of pharmaceutical and biomedical research.

■ ASSOCIATED CONTENT

Supporting Information

Absorbance and FL spectra, DLS, AFM investment of polymer micelles. This material is available free of charge via the Internet at http://pubs.acs.org.

■ AUTHOR INFORMATION

Corresponding Author

*E-mail: jiangjq@snnu.edu.cn. Tel.: 86-29-81530784. Fax: 86-29-81530784.

Notes

The authors declare no competing financial interest.

■ ACKNOWLEDGMENTS

This work is supported by the Nature Science Foundation of China (NSFC 21374056), Program for Changjiang Scholars and Innovative Research Team in University (IRT-14R33), the Natural Science Basic Research Plan in Shaanxi Province of China (NSBRP-SPC 2014JM2051), the Fundamental Research Funds for the Central Universities (GK201302045), Shaanxi Innovative Research Team for Key Science and Technology (2012KCT-21, 2013KCT-17), and the One Hundred Plan of Shaanxi Province.

■ REFERENCES

(1) Discher, D. E.; Eisenberg, A. Polymer Vesicles. *Science* **2002**, *9*, 967−973.
(2) Haag, R. Supramolecular Drug-Delivery Systems Based on Polymeric Core-Shell Architectures. *Angew. Chem., Int. Ed.* **2004**, *43*, 278−282.
(3) Jiang, J. Q.; Tong, X.; Zhao, Y. A New Design for Light-Breakable Polymer Micelles. *J. Am. Chem. Soc.* **2005**, *127*, 8290−8291.
(4) Jiang, J. Q.; Qi, B.; Lepage, M.; Zhao, Y. Polymer Micelles Stabilization on Demand through Reversible Photo-Cross-Linking. *Macromolecules* **2007**, *40*, 790−792.
(5) Kabanov, A. V.; Vinogradov, S. V. Nanogels as Pharmaceutical Carriers: Finite Networks of Infinite Capabilities. *Angew. Chem., Int. Ed.* **2009**, *48*, 5418−5429.
(6) Wang, X. R.; Liu, G. H.; Hu, J. M.; Zhang, G. Y.; Liu, S. Y. Concurrent Block Copolymer Polymersome Stabilization and Bilayer Permeabilization by Stimuli-Regulated "Traceless" Crosslinking. *Angew. Chem., Int. Ed.* **2014**, *53*, 3138−3142.
(7) Duncan, R. The Dawning Ere Of Polymer Therapeutics. *Nat. Rev. Drug Discovery* **2003**, *2*, 347−360.
(8) Guo, A.; Liu, G.; Tao, J. Star Polymers and Nanospheres from Cross-Linkable Diblock Copolymers. *Macromolecules* **1996**, *29*, 2487−249.
(9) Thurmond, K. B.; Kowalewski, T.; Wooley, K. L. Water-Soluble Knedel-like Structures: The Preparation of Shell-Cross-Linked Small Particles. *J. Am. Chem. Soc.* **1996**, *118*, 7293−7240.
(10) Lavasanifar, A.; Samuel, J.; Kwon, G. S. Poly(Ethylene Oxide)-*block*-Poly(L-Amino Acid) Micelles for Drug Delivery. *Advanced Drug Deliver. Rev.* **2002**, *54*, 169−190.
(11) Savic, R.; Eisenberg, A.; Maysinger, D. Block Copolymer Micelles as Delivery Vehicles of Hydrophobic Drugs: Micelle−Cell Interactions. *J. Drug Target.* **2006**, *14* (6), 343−355.
(12) Letchford, K.; Liggins, R.; Burt, H. Solubilization of Hydrophobic Drugs by Methoxy Poly(Ethylene Glycol)-Block-Polycaprolactone Diblock Copolymer Micelles: Theoretical and Experimental Data and Correlations. *J. Pharm. Sci.* **2008**, *97* (3), 1179−1190.
(13) Kim, S.; Shi, Y. Z.; Kim, J. Y.; Park, K.; Cheng, J.-X. Overcoming the Barriers in Micellar Drug Delivery: Loading Efficiency, in vivo Stability, and Micelle-Cell Interaction. *Expert Opin. Drug Delivery* **2010**, *7* (1), 49−62.
(14) Gaucher, G.; Dufresne, M.-H.; Sant, V. P.; Kang, N.; Maysinger, D.; Leroux, J.-C. Block Copolymer Micelles: Preparation, Characterization and Application in Drug Delivery. *J. Controlled Release* **2005**, *109*, 169−188.
(15) Jiwpanich, S.; Ryu, J.-H.; Bickerton, S.; Thayumanavan, S. Noncovalent Encapsulation Stabilities in Supramolecular Nanoassemblies. *J. Am. Chem. Soc.* **2010**, *132*, 10683−10685.
(16) Argentiere, S.; Blasi, L.; Morello, G.; Gigli, G. A Novel pH-Responsive Nanogel for the Controlled Uptake and Release of Hydrophobic and Cationic Solutes. *J. Phys. Chem. C* **2011**, *115*, 16347−16353.
(17) Bickerton, S.; Jiwpanich, S.; Thayumanavan, S. Interconnected Roles of Scaffold Hydrophobicity, Drug Loading, and Encapsulation Stability in Polymeric Nanocarriers. *Mol. Pharmaceutics* **2012**, *9*, 3569−3578.
(18) Ryu, J.-H.; Chacko, R. T.; Jiwpanich, S.; Bickerton, S.; Babu, R. P.; Thayumanavan, S. Self-Cross-Linked Polymer Nanogels: A Versatile Nanoscopic Drug Delivery Platform. *J. Am. Chem. Soc.* **2010**, *132*, 17227−17235.
(19) Bae, Y. H.; Yin, H. Stability Issues of Polymeric Micelles. *J. Controlled Release* **2008**, *131*, 2−4.
(20) Hong, S. W.; Kim, K. H.; Huh, J.; Ahn, C.-H.; Jo, W. H. Design and Synthesis of a New pH Sensitive Polymeric Sensor Using Fluorescence Resonance Energy Transfer. *Chem. Mater.* **2005**, *17* (25), 6214−6215.
(21) Yan, L.; Hang, C.; Jiang, J. Q.; Yan, X. Y.; Liu, Z. T.; Liu, Z. W. The Photodimerization Characteristics of Anthracene Pendants within Amphiphilic Polymer Micelles in Aqueous solution. *RSC Adv.* **2014**, *4*, 25912−25915.
(22) Jiang, J. Q.; Feng, Y.; Wang, H. M.; Liu, X. Y.; Zhang, S. W.; Chen, M. Q. Synthesis and Micellization of Photosensitive Amphiphilic Comblike SMA Polymer. *Acta Phys. Chim. Sin.* **2008**, *24*, 2089−2095.
(23) Mal, N. K.; Fujiwara, M.; Tanaka, Y. Photocontrolled Reversible Release of Guest Molecules from Coumarin-Modified Mesoporous Silica. *Nature* **2003**, *421*, 350−353.

(24) He, J.; Yan, B.; Tremblay, L.; Zhao, Y. Both Core- and Shell-Cross-Linked Nanogels: Photoinduced Size Change, Intraparticle LCST, and Interparticle UCST Thermal Behaviors. *Langmuir* **2011**, *27*, 436−444.
(25) Guo, Z. X.; Jiao, T. F.; Liu, M. H. Effect of Substituent Position in Coumarin Derivatives on the Interfacial Assembly: Reversible Photodimerization and Supramolecular Chirality. *Langmuir* **2007**, *23*, 1824−1829.
(26) Schraub, M.; Soll, S.; Hampp, N. High Refractive Index Coumarin-Based Photorefractive Polysiloxanes. *Eur. Polym. J.* **2013**, *49*, 1714−1721.
(27) Kihara, H.; Yoshida, M. Reversible Bulk-Phase Change of Anthroyl Compounds for Photopatterning Based on Photodimerization in the Molten State and Thermal Back Reaction. *ACS Appl. Mater. Interfaces* **2013**, *5*, 2650−2657.
(28) Wang, C.; Zhang, D. Q.; Xiang, J. F.; Zhu, D. B. New Organogels Based on an Anthracene Derivative with One Urea Group and Its Photodimer: Fluorescence Enhancement after Gelation. *Langmuir* **2007**, *23*, 9195−9200.
(29) Al-Kaysi, R. O.; Bardeen, C. J. Reversible Photoinduced Shape Changes of Crystalline Organic Nanorods. *Adv. Mater.* **2007**, *19*, 1276−1280.
(30) Ye, X. L.; Jiang, X. S.; Yu, B.; Yin, J.; Vana, P. Functional Binary Micropattern of Hyperbranched Poly(ether amine) (hPEA-AN) Network and Poly(ether amine) (PEA) Brush for Recognition of Guest Molecules. *Biomacromolecules* **2012**, *13*, 535−541.
(31) Jezowski, S. R.; Zhu, L. Y.; Wang, Y. B.; Rice, A. P.; Scott, G. W.; Bardeen, C. J.; Chronister, E. L. Pressure Catalyzed Bond Dissociation in an Anthracene Cyclophane Photodimer. *J. Am. Chem. Soc.* **2012**, *134*, 7459−7466.
(32) Chen, W.; Wang, J. Y.; Li, L.; Balazs, A. C.; Matyjaszewski, K.; Russell, T. P. Photocontrol over the Disorder-to-Order Transition in Thin Films of Polystyrene-block-poly(methyl methacrylate) Block Copolymers Containing Photodimerizable Anthracene Functionality. *J. Am. Chem. Soc.* **2011**, *133*, 17217−17224.
(33) Su, Z. L.; Yu, B.; Jiang, X. S.; Yin, J. Responsive Fluorescent Nanorods from Coassembly of Fullerene (C_{60}) and Anthracene-Ended Hyperbranched Poly(ether amine) (AN-hPEA). *Macromolecules* **2013**, *46*, 3699−3707.
(34) Xu, J. F.; Chen, Y. Z.; Wu, L. Z.; Tung, C. H.; Yang, Q. Z. Dynamic Covalent Bond Based on Reversible Photo [4+4] Cycloaddition of Anthracene for Construction Of Double-Dynamic Polymers. *Organic Lett.* **2013**, *15*, 6148−6151.
(35) Zheng, Y. J.; Micic, M.; Mello, S. V.; Mabrouki, M.; Andreopoulos, F. M.; Konka, V.; Pham, S. M.; Leblanc, R. M. PEG-Based Hydrogel Synthesis via the Photodimerization of Anthracene Groups. *Macromolecules* **2002**, *35*, 5228−5234.
(36) Kokotos, G.; Tzougraki, C. Synthesis and Study of Substituted Coumarins. A Facile Preparation of D, L-*o*-tyrosine. *J. Heterocycl. Chem.* **1986**, *23*, 87−92.
(37) Guy, J.; Caron, K.; Dufresne, S.; Michnick, S. W.; Skene, W. G.; Keillor, J. W. Convergent Preparation and Photophysical Characterization of Dimaleimide Dansyl Fluorogens: Elucidation of the Maleimide Fluorescence Quenching Mechanism. *J. Am. Chem. Soc.* **2007**, *129*, 11969−11977.
(38) Ranjit, S.; Levitus, M. Probing the Interaction Between Fluorophores and DNA Nucleotides by Fluorescence Correlation Spectroscopy and Fluorescence Quenching. *Photochem. Photobiol.* **2012**, *88*, 782−791.
(39) Atherton, J. C. C.; Jones, S. Diels−Alder Reactions of Anthracene, 9-Substituted Anthracenes and 9, 10-Disubstituted Anthracenes. *Tetrahedron* **2003**, *59*, 9039−9057.
(40) Gacal, B.; Durmaz, H.; Tasdelen, M. A.; Hizal, G.; Tunca, U.; Yagci, Y.; Demirel, A. L. Anthracene-Maleimide-Based Diels−Alder "Click Chemistry" as a Novel Route to Graft Copolymers. *Macromolecules* **2006**, *39*, 5330−5336.
(41) Helm, M.; Petermeier, M.; Ge, B.; Fiammengo, R.; Jäschke, A. Allosterically Activated Diels−Alder Catalysis by a Ribozyme. *J. Am. Chem. Soc.* **2005**, *127*, 10492−10493.